Applied Clay Science 135 (2017) 52–63

Contents lists available at ScienceDirect

Applied Clay Science

journal homepage: www.elsevier.com/locate/clay

Research paper

Preparation, characterization and application in controlled release of Ibuprofen-loaded Guar Gum/Montmorillonite Bionanocomposites

Joanna Dziadkowiec [a,b,*], Rola Mansa [a], Ana Quintela [b], Fernando Rocha [b], Christian Detellier [a]

[a] Centre for Catalysis Research and Innovation and Department of Chemistry, University of Ottawa, 10 Marie Curie, Ottawa, Ontario K1N 6N5, Canada
[b] Geobiotec RC, Geosciences Department, University of Aveiro, Campus Universitário de Santiago, 3810-193 Aveiro, Portugal

ARTICLE INFO

Article history:
Received 27 June 2016
Received in revised form 30 August 2016
Accepted 3 September 2016
Available online 13 September 2016

Keywords:
guar gum
montmorillonite
bionanocomposites
Ibuprofen
in vitro release
Portuguese clay
CPN
smectite
nanocomposites

ABSTRACT

Neutral guar gum-montmorillonite and cationic guar gum-montmorillonite nanocomposites loaded with ibuprofen were prepared, and their ability to control *in vitro* release of the drug was presented. These materials exhibited a reduced initial burst release effect and sustained release of up to several hours in a pH 7.4 simulated intestinal fluid. Blank experiments suggested a nanocomposite-mediated action. Improved properties were demonstrated for two different clay minerals: Sodium Wyoming (SWy-2) montmorillonite from the Source Clay Repository and a Portuguese montmorillonite from the Benavila bentonite deposit. The prepared materials were based on abundant, low-cost, natural minerals and plant-extracted biopolymers, and were synthesized using a facile method, thus exhibiting a low environmental impact.

1. Introduction

Clay minerals are ubiquitous near the Earth's surface and offer remarkable potentials in material science (Bergaya and Lagaly, 2013). Among others, clay-polymer nanocomposites (CPN) are extensively investigated across disciplines (Bergaya et al., 2013). Currently, there is an urgent need to seek advanced functional materials with low environmental impact, which generates a strong interest in biopolymers. Clay-biopolymer nanocomposites are a novel class of versatile materials with an expanding range of possible applications involving drug delivery systems and tissue engineering (Dawson and Oreffo, 2013; Lambert and Bergaya, 2013; Ruiz-Hitzky et al., 2013; Mansa et al., 2015). Smectite is the most common clay mineral component of these materials (Lambert and Bergaya, 2013).

Montmorillonite (Mt) belongs to the smectite group, which comprises the 2:1 layer type, swelling clay minerals with relatively low layer charge (0.3 to 0.6 per half unit cell - $O_{10}[OH]_2$) (Velde and Meunier, 2008). In particular, Mt is a dioctahedral smectite with heterovalent substitutions in octahedral sheets ($Mg^{2+} \rightarrow Al^{3+}$) and the typical chemical formula - $(Na,Ca)_{0.3}(Al,Mg)_2Si_4O_{10}[OH]_2 \cdot n(H_2O)$.

Medicinal properties of clays have been recognized since ancient times (Young et al., 2011; Gomes et al., 2013), and up till now, raw clays and clay minerals have been used in pharmaceutical formulations as active agents and excipients. Due to their cation exchange capacity and adsorptive potential, they can interact with drug molecules, facilitating their liberation. Sustained release of drugs, controlled by desorption from clay mineral excipients, was found favorable in the case of antibiotics, amphetamines and anti-inflammatory drugs (Mcginity and Lach, 1977; Porubcan et al., 1978; Zheng et al., 2007; Gomes et al., 2013). Carretero and Pozo (2009) describe advantageous rheological, colloidal, thixotropic, mechanical and bioadhesive properties of clay mineral excipients. By making the gastric mucus more viscous and stable, clay minerals can act as gastrointestinal protectors against aggressive agents, such as pepsin and some anti-inflammatory drugs (More et al., 1987; Droy-Lefaix and Tateo, 2006). Smectite was demonstrated to be efficient in alleviating ailments caused by ingestion of non-steroidal anti-inflammatory drugs (Droy-Lefaix and Tateo, 2006).

Guar gum is a galactomannan biopolymer of high molecular weight, extracted from endosperm of guar plant's seeds (Mathur, 2011). It is a copolymer of mannose and galactose, comprised of a linear backbone of D-mannopyranose units, linked through β(1→4) glycosidic bonds. D-galactopyranose grafts are side-chained to mannose units at the C-6 position by α(1→6) glycosidic bonds. One derivative of guar gum is

* Corresponding author at: Physics of Geological Processes (PGP), University of Oslo, P.O. Box 1048, Blindern, N-0316 Oslo, Norway.
E-mail addresses: joanna.dziadkowiec@fys.uio.no (J. Dziadkowiec), rmansa@uottawa.ca (R. Mansa), anaquintela@ua.pt (A. Quintela), tavares.rocha@ua.pt (F. Rocha), Christian.Detellier@uottawa.ca (C. Detellier).

http://dx.doi.org/10.1016/j.clay.2016.09.003
0169-1317/

guar 2-hydroxy-3-(trimethylammonio)propyl ether chloride (cationic guar gum), modified with a quaternary ammonium cation. Guar gum and its derivatives are manufactured at an industrial scale and primarily serve as highly viscous food hydrocolloids. Cationic guar gum has extensive use in cosmetics, where it serves as a viscosity, volume and foam enhancer. Guar gum is used in pharmaceutical formulations and as an excipient with drug release controlling properties due to its non-toxicity, biodegradability, low cost and useful physicochemical properties (Mathur, 2011). Moreover, it is reported to be therapeutically active (Alam et al., 2000; Chaurasia et al., 2006; Gamal-Eldeen et al., 2006; Butt et al., 2007; Belo et al., 2008; Kuo et al., 2009; Takahashi et al., 2009). Native and chemically modified guar gum has been proposed to serve as a cost-effective matrix and a coating in colonic and retarded delivery of various drugs, as indicated by numerous in vitro and in vivo studies (Altaf et al., 1998; Prasad et al., 1998; Soppimath et al., 2001; Krishnaiah et al., 2002a, 2002b; Chourasia and Jain, 2004; Toti and Aminabhavi, 2004; Sen et al., 2010; Tiwari and Prabaharan, 2010; Prabaharan, 2011; Tripathy et al., 2013; Singh et al., 2014, Seeli and Prabaharan, 2016).

Biopolymers become adsorbed and intercalated in the interlayer space of smectite clay minerals, driven by electrostatic interactions or by a gain in the system's entropy (Henao and Mazeau, 2009; Theng, 2012). As a result, clay minerals may undergo delamination leading eventually to exfoliation giving rise to CPN. In such materials, clay mineral layers act as a nanometer-sized phase domain associated with a polymeric matrix (Theng, 2012; Bergaya and Lagaly, 2013). Such a unique structure may induce modulated release of the drug due to the interaction with both the polymer and the clay mineral. The potential use of the guar gum-Mt nanocomposites in drug delivery applications was suggested by Mansa and Detellier (2013).

Ibuprofen (IBU) is a non-steroidal, anti-inflammatory drug with analgesic and antipyretic properties. However, treatment with (IBU) frequently leads to side effects, due to the reported gastrointestinal toxicity of this drug (Lichtenstein et al., 1995). IBU contributes to topical injuries of the gastric mucus, what decreases mucus resistance to acidic environment, pepsin and some exogenous factors, such as the drug itself (Wolfe et al., 1999). Additionally, IBU has an adverse systemic effect on gastric, mucosal protective agents (Schoen and Vender, 1989). Another problematic issue is related to the fast absorption of the drug (maximum blood concentration levels of IBU are reached within 1-2 h) and its rapid elimination from the plasma (~2 h) (Wilson et al., 1989).

Due to its short half-life and adverse gastrointestinal side effects, modified drug delivery systems for IBU are desired. Such systems should exhibit sustained release of the drug so as to: decrease dosing frequency, prevent reaching toxic concentration of drug in the body, hinder unsteady release, and minimize occurrence of side effects (Wilson et al., 1989; Arida et al., 1999). Several authors report modified IBU delivery systems, based on polymers (Das et al., 2006; Pang et al., 2011; Abdeen and Salahuddin, 2013; Seeli et al., 2016), clay minerals (Zheng et al., 2007); halloysite nanotubes (Tan et al., 2013, 2014; Yuan et al., 2015); LDH (Rojas et al., 2012), zeolites (Horcajada et al., 2006), and CPN (Depan et al., 2009; Campbell et al., 2010). However, to the best of our knowledge, there are no such systems based on guar gum-Mt nanocomposites, which are attractive due to high adsorptive potential and cation exchange capacity of the clay mineral component, as well as intercalation of guar gum. The latter contributes to an increase of montmorillonite interlayer space, potentially contributing to further intercalation of drug molecules, which can also interact with guar gum's functional –OH groups. Mt in particular is advantageous for use in preparing nanocomposites with water-soluble polysaccharides due to its hydrophilicity and its dispersibility in water. Additionally, the use of Mt from a raw bentonite deposit can give substantial insight into clay mineral-polymer interactions, which are usually studied using commercial clay products and reference clay minerals.

2. Materials and Methods

2.1. Materials

Raw Portuguese Mt from the Benavila bentonite deposit (BV3) and the reference clay mineral, Sodium Wyoming Mt (SWy-2), were used to prepare the CPN. BV3 was collected from the Benavila bentonite deposit located in the central-east part of Portugal, close to Benavila town, which belongs to Portalegre district (-7.8522 W and 39.1275 N at the altitude of 158 m.a.s.l.). Typically, about 1kg of BV3 was purified using a wet sieving procedure. SWy-2 was supplied from the Source Clay Repository (the Clay Minerals Society, USA). Clay fraction (<2 μm) was achieved from both the BV3 and SWy-2 clays by a sedimentation procedure according to Stokes Law. The amount of clay fraction for the BV3 sample was determined by an X-ray beam particle size analyzer (Micromeritics® Sedigraph 5100). Subsequently, to enhance their swelling properties (Norrish and Quirk, 1954) Mt samples were saturated with Na^+ according to a procedure adapted from Carrado et al. (2006). Clay samples were then washed with distilled water and recovered by centrifugation (10 000 rpm). After washing, dialysis was performed to remove excess salts (using dialysis membranes from Spectrum Laboratories Inc., MCWO 12,000 – 14,000) until no Cl^- was detected by $AgNO_3$ test. The samples were dried at 60°C and ground with an agate mortar and a pestle. The sodium saturated samples were labelled Na^+-SWy and Na^+-BV3.

Neutral guar gum (NGG) was purchased from Sigma-Aldrich (USA). It has a total ash content <1% and loss on drying < 13%. Cationic guar gum (gum guar 2-hydroxy-3-(trimethylammonio)propyl ether chloride, CGG) with N content ranging from 0.8 – 1.8% was purchased from Spec-Chem Ind. (China). Both gums were used as received.

Ibuprofen (α-Methyl-4-(isobutyl)phenylacetic acid) sodium salt ≥98% with a molecular formula $C_{13}H_{17}O_2Na$ and a molecular weight of 228.3 g/mol, was supplied from Sigma-Aldrich and used as received (See Fig. 1).

2.2. Methods

2.2.1. Preparation of Ibuprofen-loaded Mt-NGG Nanocomposite

The IBU/SWy-NGG, having NGG : IBU sodium salt: Na^+-SWy mass ratio of 6 : 2 : 1 was prepared using the following procedure: 0.7 g of Na^+-SWy were dispersed in 600 mL of distilled water. Subsequently, 1.4 g of IBU sodium salt were added to the clay mineral dispersion, followed by the addition of 4.2 g of NGG. The mixture was stirred magnetically (1500 rpm) at room temperature for 2 weeks. Some part of the material was removed at that point, dried at 50°C and ground with an agate mortar (labeled as IBU/SWy-NGG-U). The remaining part was recovered by centrifugation at 5000 rpm for 5 min, the supernatant was discarded, and the sample was dried at 50°C and ground with an agate mortar, without further washing (labeled as IBU/SWy-NGG). The high NGG to Na^+-SWy ratio was chosen to enhance delamination of the clay mineral (Mansa and Detellier, 2013).

2.2.2. Preparation of Ibuprofen-loaded CGG-Mt Nanocomposites

The IBU/SWy-CGG and IBU/BV3-CGG nanocomposites, having CGG : IBU sodium salt: Mt mass ratio of 4 : 2: 1, were prepared using the following procedure. 0.5 g of Na^+-SWy or Na^+-BV3 were dispersed in 1L of distilled water prior to addition of 1.0 g of IBU sodium salt. After 30 min, 2.0 g of CGG were added to the dispersions and stirred 3 days at 500 rpm, at room temperature. The unwashed samples, labeled IBU/SWy-CGG-U and IBU/BV3-CGG-U were then dried at 50°C and ground with agate mortar. Subsequently, a portion of both materials was washed with water. Typically, ~1.5 g of the samples were dispersed in 200 mL of distilled water, shaken vigorously in a centrifuge bottle and centrifuged at 5000 rpm for 5 min. The samples were dried at 50°C and ground with an agate mortar. The resulting materials are referred to as IBU/SWy-CGG and IBU/BV3-CGG.

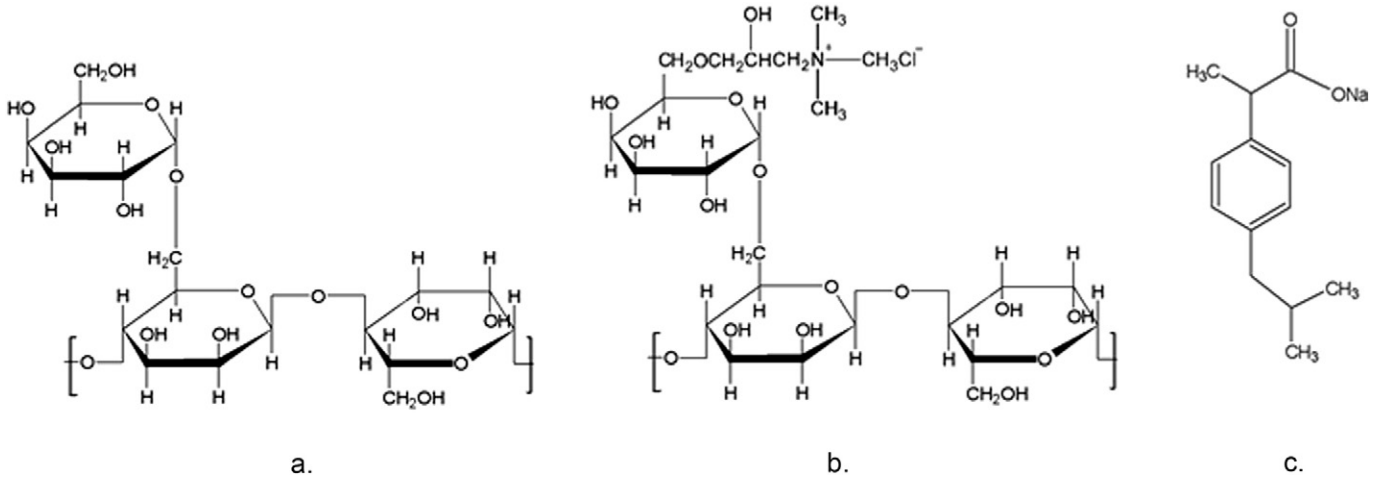

Fig. 1. Structures of: a. NGG, b. CGG, c. IBU sodium salt.

2.2.3. Preparation of Blank Guar Gum-Mt Nanocomposites

As a reference, similar nanocomposite materials were prepared without IBU. Na^+-SWy NGG nanocomposite (SWy-NGG), with a biopolymer to clay mineral ratio of 6 : 1, was prepared by a solvent intercalation method (distilled water) adapted from Mansa and Detellier (2013).

Mt-CGG nanocomposites, with a biopolymer to clay mineral ratio of 4 : 1, were prepared by a solvent intercalation method using a modified procedure adapted from Mansa and Detellier (2013). Prior to addition of CGG, 0.5 g of dry sodium-saturated Mt (Na^+-BV3 or Na^+-Swy) were dispersed in 1L of distilled water to allow swelling. Subsequently, 2 g of CGG were added into the clay dispersion and stirred for 3 days at 500 rpm, at room temperature. The materials were dried at 50°C, well-ground with an agate mortar and labelled SWy-CGG and BV3-CGG respectively.

2.2.4. Preparation of Ibuprofen Blank Samples

The IBU/SWy blank was prepared keeping the IBU sodium salt to Mt ratio of 2 : 1. Typically, 0.25 g of Na^+-SWy were dispersed in 0.5 L of distilled water, prior to addition of 0.5 g of IBU sodium salt. The dispersion was stirred for 3 days using a magnetic stirrer (500 rpm) at room temperature. Subsequently, the product, labeled as IBU/SWy-U, was dried at 50°C and ground with an agate mortar. Additionally, a similar material was prepared using the above procedure, where prior to drying, the material was centrifuged at 10 000 rpm for 5 min. The supernatant was discarded, and the recovered Mt was dried at 50°C, ground with an agate mortar and labeled as IBU/SWy.

The IBU/NGG and IBU/CGG blank samples were prepared maintaining the guar gum to IBU sodium salt mass ratio as previous experiments, 3:1 and 2:1, respectively. Typically, 200 mg of NGG and 66 mg of IBU sodium salt were dissolved in 100 mL of distilled water. Similarly, 200 mg of CGG and 100 mg of IBU sodium salt were dissolved in 100 mL of distilled water. Both samples were shaken for 3 days on a platform shaker (300 rpm) at room temperature. Subsequently, the samples were dried at 50°C and ground with an agate mortar.

In addition, physical mixtures of IBU/SWy-NGG and IBU/SWy- were prepared keeping the same mass ratio of the drug, the biopolymer and the clay mineral as in the corresponding CPN.

2.3. Characterization of the Samples

The mineralogical composition of the Benavila bentonite sample (fraction <63 μm) was determined using a Philips/Panalytical X'pert-Pro MPD, with Cu Kα radiation (λ = 1,5405 Å), and a step size of 0,02° 2θ s^{-1}, in the 2θ angle range 4-65°. The randomly oriented powder mount was prepared by a back-loading method. The identification of clay minerals was carried out using oriented aggregates. Dispersions of the clay fraction <2 μm, were deposited on thin glass slides and air dried. Diffraction patterns were measured with a step size 0,02° in the 2θ angle range 4-20°. Afterwards, diffractograms of the slides, saturated with ethylene glycol (24 h), and heated to 500°C, were recorded in order to differentiate between particular clay minerals. Semi-quantification of mineralogical composition was performed by a method adapted from Martins et al. (2007), and verified using the results of X-ray fluorescence spectroscopy (XRF) chemical analysis.

X-ray diffractograms of the synthesized CPN were collected using Philips PW 3710 diffractometer, with a Cu Kα radiation at 45 kV, 40 mA, and with a step size of 0,02°2θ, in 2-90° 2θ angle range. Randomly oriented powder samples were prepared by a back-loading method. Oriented XRD mounts were prepared by pipetting a small amount of dispersion onto glass slides, which were then air dried.

The chemical composition of the Benavila bentonite (BV3, fractions <63 μm and <2 μm) was determined by XRF using a Philips Panalytical PW1404 X-ray fluorescence wavelength dispersive spectrometer for major, minor and trace elements. Routinely, for the analysis, a pressed powder pellet was made out of about 12 g of the sample.

Scanning electron microscopy was performed for the Benavila Mt sample (BV3, fraction <2 μm) using a Hitachi SEM S-4100 scanning electron microscope equipped with Bruker Quantax 400 Energy Dispersive Spectrometer (EDS) for point chemical analyses, without sample coating. The SEM images were acquired with a tungsten filament working at 20 kV and the EDS was performed at 15 kV in order to determine smectite type in the sample and calculate its estimated chemical formula (as an average result of five point measurements recalculated with respect to charge balance).

Cation exchange capacity (CEC) was determined as a sum of exchangeable cations after saturation with ammonium cations. Typically, about 5.0 g of a clay sample, dried at 50°C was dispersed in a 1M ammonium acetate solution for 24h and, thus, saturated with NH_4^+ cations. Afterwards, the clay sample was separated by filtration using a glass fiber filter paper (Macherey-Nagel MN640d). At this point, 100 mL of the filtrate was collected and analyzed by inductively coupled plasma mass spectrometry for quantitative determination of exchangeable cations using Agilent 7700 X Spectrometer.

Thermogravimetric data (TG, DTG) were recorded using a TGA Q5000 instrument in a temperature range of ~30°C – 700°C or ~30°C – 1000 °C and a heating rate of 10°C/min, under nitrogen atmosphere. Platinum-HT or alumina Al_2O_3 sample pans were used and the amount of a sample was ranging from ~2 mg – 15 mg.

2.4. Determination of Drug Loading

The content of IBU was determined by using a modified method adapted from Wang et al. (2009) and Ribeiro et al. (2014). Typically, 20 mg of a drug loaded material were placed in a plastic tube, which was then filled with 50 mL of phosphate buffer (pH 7.4), prepared according to U.S. Pharmacopeia (Buffer Solutions). The tube was shaken for 3 days (300 rpm), at room temperature. Subsequently, the solution was sonicated using a constant pulse program for 5 minutes and filtered using a qualitative paper filter. The tube was filled again with a known amount of fresh phosphate buffer in order to rinse it, and this solution was filtered, too. The experiment was performed in triplicate for each sample. The concentration of the IBU was measured in the collected filtrate using a Genesys10S UV-Vis Spectrometer and a quartz cuvette at $\lambda_{max} = 222$ nm. UV-Vis measurements were carried out in triplicate, as well. The error was expressed as a standard deviation.

Drug loading (DL) and drug loading efficiency (DLE) were calculated according to the following equations (Ambrogi et al., 2008):

$$\%DL = \frac{mass\ of\ drug\ in\ the\ material\ [mg]}{mass\ of\ the\ material\ [mg]} * 100\%$$

$$\%DLE = \frac{mass\ of\ drug\ loaded = DL\ of\ the\ treated\ sample\ [mg]}{total\ mass\ of\ drug\ added = DL\ of\ the\ untreated\ sample\ [mg]} * 100\%$$

2.5. In Vitro Release Experiments

In vitro release experiments were performed using a modified membrane dissolution method, adapted from Marchal-Heussler et al. (1990) and Shen and Burgess (2013). The experiments were carried out, using simulated intestinal fluid (SIF) - phosphate buffer pH = 7.4, as a release medium. The buffer was prepared according to U.S. Pharmacopeia by mixing 250 mL of 0.2M KH_2PO_4, 195.5 mL of 0.2 M NaOH and adding distilled water to equal a volume of 1L. Cellulose dialysis membranes, with MCWO 12,000 – 14,000, were supplied from Spectrum Laboratories Inc. Prior to release experiments, the membranes were immersed in distilled water for 2h to remove any preservatives, rinsed thoroughly with water and immersed in the SIF to equilibrate for 1h. Subsequently, the dialysis bag was filled with 6 mL of the release medium. Afterwards, the carefully weighed amount of a powdered material, that contained approximately 20 mg of IBU, was placed inside the membrane. The bag, sealed with plastic clips, was shaken and immediately immersed in the 300 mL of the release medium, which was pre-heated to 37°C in order to simulate body temperature. The experiments were performed using a magnetic stirrer (100 rpm), during a 6h-interval. The aliquots of 9 mL (3 x 3 mL) were withdrawn at fixed time interval and replaced with 9 mL of a fresh release medium each time. The concentration of IBU was measured by UV-Vis Spectroscopy in triplicates, using a Genesys10S UV-Vis single beam spectrometer at λ = 222 nm, using pH 7.4 phosphate buffer as a solvent.

3. Results and Discussion

3.1. Mineralogical and Chemical Composition of the Benavila Mt (BV3)

The Benavila bentonite, sampled in the Hercynian Massif, is a residual rock that originated from the weathering of Benavila granodiorites. This alteration product can be dated as a paleogenic deposit (Rebelo et al., 2010) and comprises Fe-rich smectite along with typical associated minerals. The grain size distribution of Benavila bentonite bulk sample, estimated from the wet sieving procedure and sedigraph analysis, indicated that the clay fraction (<2 μm) constitutes approximately 30% of the raw sample. XRD analysis revealed the BV3 sample (<63 μm) to be mainly composed of smectite (76%) and calcite (21%) as a main associated mineral phase (Table 1). The purified BV3 sample (<2 μm) was enriched in smectite (>90%) as indicated by XRD semi-quantification. The XRF chemical composition of the BV3 sample (<63 μm), regarding the major elements, is in a good agreement with their mineralogical composition. High abundance of Si and Al (SiO_2 ~50%, Al_2O_3 ~15%) is linked with the main mineral phases: Si-rich phyllosilicates and primary silicates. Presence of Fe in major amounts (Fe_2O_3 ~10%) may be attributed to Fe-rich smectite and amorphous or poorly crystalline Fe-(hydr)oxides, undetectable by XRD. The dominant source of Ca is calcite, which is well reflected by substantial loss on ignition, mainly caused by water loss and very likely carbonate decomposition. XRF analysis of the clay fraction (<2 μm) indicated that the BV3 sample was enriched in Si, Al, Fe and Mg and depleted in Ca as compared to the silt-clay fraction (<63 μm), and confirmed that smectite content was increased. Additionally, ~7% CaO depletion indicated a partial removal of calcite impurity. Among the minor elements, relatively high content of chromium may be linked with the sample residual origin (alteration of magmatic rocks – granodiorites, containing Cr-bearing minerals) (Oze et al., 2007). According to U.S Pharmacopeial Convention (2012), Cr is not considered dangerous in pharmaceutical formulations. Additionally, the bioaccessible fraction of potentially harmful elements, such as Cr, that reaches the human or animal systemic circulation is usually much lower than their total concentration in the clay (Stewart et al., 2003; Van de Wiele et al., 2007; Roussel et al., 2010; Wragg et al., 2011).

The smectite type in the sample was determined by XRD and SEM-EDS analyses. Dioctahedral and trioctahedral smectites can be distinguished on the basis of smectite (060) XRD reflection's position (Brindley and Brown, 1980). The smectite type present in BV3 sample is a dioctahedral one (the (060) reflection was measured at 1.505 Å). The average chemical formula of the BV3 is $Mg_{0.08}Ca_{0.08}Na_{0.04}K_{0.03}(Al_{1.18}Fe_{0.44}Mg_{0.38})O_{10}(Si_{3.99}Al_{0.01})(OH)_2 \cdot nH_2O$, as recalculated from the SEM-EDS results, and it corresponds to Mt.

XRD patterns of the commercial Wyoming Mt from the Source Clay Repository (SWy-2) and Portuguese Mt (BV3) after purification and saturation with Na^+ are presented in Fig. 2. Quartz (~10%) is present as an impurity in the Na^+-SWy sample. In the case of Na^+-BV3, there is a trace amount of calcite. Effective CEC, calculated as a sum of exchangeable cations, is equal to 61 cmol(+)/kg for the Na^+-SWy and 111 cmol(+)/kg for the Na^+-BV3.

3.2. Drug Loading and Structure of Nanocomposites

3.2.1. IBU/SWy Blank Samples

Interaction of IBU with Mt was studied using XRD and TGA (Figs. 3, 4). The XRD pattern of the untreated blank IBU/SWy-U indicated a significant enhancement of the d-value from 12.5 Å to 15.0 Å, suggesting intercalation of IBU into the clay mineral interlayer. IBU-intercalated Mt complexes were also obtained by Zheng et al. (2007), where the clay mineral d-value varied from 13.2 Å to 15.7 Å, depending on the

Table 1
Mineralogical composition of the BV3 sample (fraction <63 μm) determined by X-ray diffraction (XRD) and X-ray fluorescence (XRF) chemical analysis of major elements and Cr in the BV3 sample (fractions <63μm and <2 μm). The results are in wt.%., *Cr content is given in ppm. (LOI – loss on ignition).

XRD % <63 μm	smectite	calcite	chlorite	K-feldspars	anatase	dolomite	quartz	plagioclases	hornblende		Fe(hydr)oxides	
	74	21	3	1	1	<1	<1	<1	<1		<1	
XRF %	SiO_2	Al_2O_3	CaO	Fe_2O_3	MgO	TiO_2	K_2O	P_2O_5	Na_2O	other	LOI	Cr*
<63 μm	45,4	14,1	9,1	9,0	5,1	0,7	0,4	0,1	0,1	0,2	15,8	480 ppm
<2 μm	52,0	15,5	2,4	10,4	5,5	0,3	0,2	0,1	0,1	0,1	13,3	460 ppm

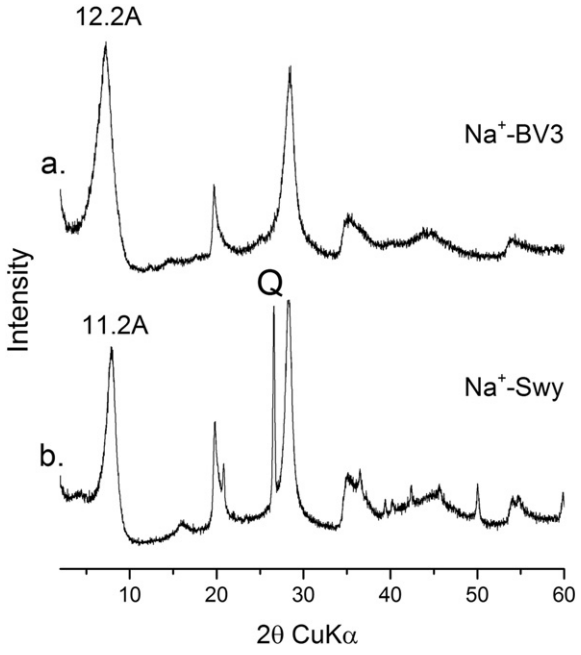

Fig. 2. X-ray diffraction (XRD) powder patterns for the purified (a) Na^+-BV3; (b) Na^+-SWy samples; clay fraction <2 μm.

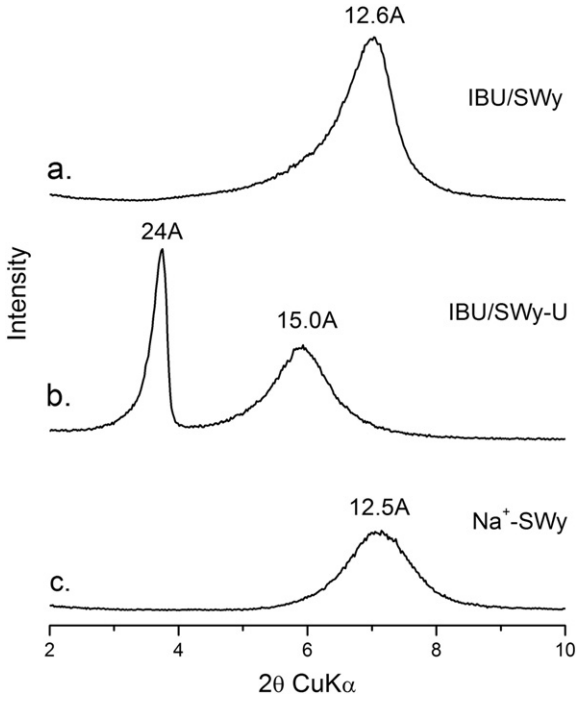

Fig. 3. X-ray diffraction (XRD) patterns (oriented aggregates) of (a) IBU/SWy; (b) IBU/SWy-U; (c) Na^+-SWy.

initial drug concentration. The intense reflection at 24 Å is due to external IBU that crystallized on the clay mineral surface. After centrifugation, the (001) reflection of IBU/SWy was reduced to 12.6 Å, which corresponds to the starting clay mineral. This indicates that the IBU that was adsorbed in the interlayer was easily replaced by water molecules. A lack of the IBU-typical reflection at 24 Å is attributed to removal of a major part of the externally adsorbed drug. Upon centrifugation, the amount of IBU was reduced from the initial 68% to 11%, showing DLE of 16% (Table 2). TGA revealed that the pyrolysis of IBU is altered upon interaction with Na^+-SWy. Whereas IBU was pyrolysed between 300°C and 500°C, indicated by the single DTG peak centered at 458°C, the DTG trace of IBU/SWy-U indicated the presence of two major peaks with maxima at 386°C and 492°C, and a shoulder at 540°C. The higher thermal stability of IBU may be attributed to its intercalation (Zheng et al., 2007). An increase in thermal stability of organic component has been reported in previous works on CPN, owing to dispersed clay layers and enhanced char formation, both acting as barriers against out-diffusion of volatile degradation products (Park et al., 2002; Leszczyńska et al., 2007; Mansa et al., 2015). As such, the DTG peaks at 386°C (IBU/SWy-U) and at 320°C (IBU/SWy) plausibly correspond to the externally absorbed part of IBU. In the case of IBU/SWy physical mixture, a vast majority of IBU was pyrolysed at temperatures typical for the drug. The altered thermal stability of IBU may be additionally influenced by changes in the drug crystallinity upon its dissolution and drying (Dubernet et al., 1990). Due to low IBU loading for the IBU/SWy sample (11%), a dehydroxylation step of Mt is detectable (a broad DTG peak centered at 665°C).

Table 2
Drug loading (DL) and drug loading efficiency (DLE) (wt.%) for the prepared samples. DLE of the untreated samples (U - not washed nor centrifuged) is considered as 100 wt.% determined by UV-Vis spectroscopy.

	Drug Loading (wt.%)	Drug Loading Efficiency (wt.%)
IBU/SWy-NGG-U	24.0 ± 0.7	-
IBU/SWy-NGG	16.5 ± 0.4	68.7
IBU/SWy-CGG -U	30.5 ± 1.1	-
IBU/SWy-CGG	15.5 ± 0.6	50.6
IBU/BV3-CGG-U	29.0 ± 0.5	-
IBU/BV3-CGG	9.6 ± 0.4	33.3
IBU/SWy-U	67.6 ± 2.2	-
IBU/SWy	11.0 ± 0.8	16.3
IBU/NGG	22.4 ± 2.5	-
IBU/CGG	29.7 ± 1.1	-

3.2.2. IBU/NGG and IBU/CGG Blank Samples

TG and DTG traces of IBU/NGG and IBU/CGG blank samples, compared to starting NGG, CGG, and IBU, showed an altered behavior of

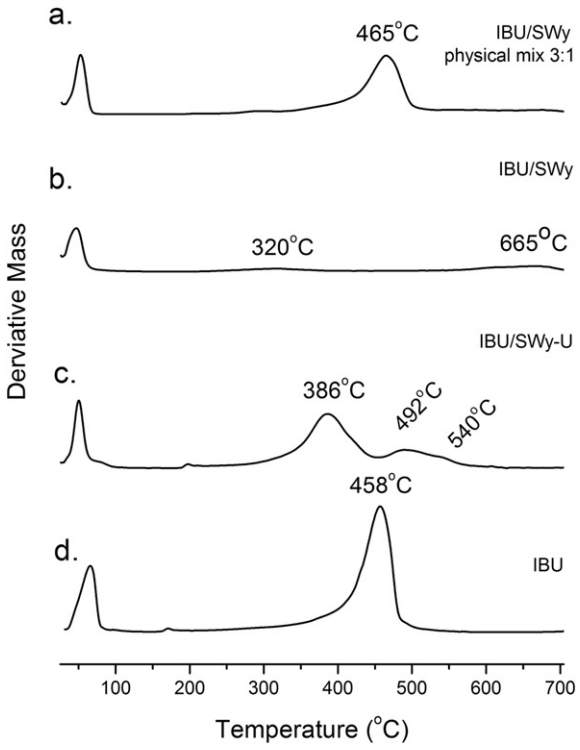

Fig. 4. Differential thermal gravimetric (DTG) traces of (a) IBU; (b) IBU/SWy-U; (c) IBU/SWy; (d) IBU/SWy physical mixture with IBU to SWy ratio 3 : 1.

both IBU and guar gum upon pyrolysis (Figs. 5, 6). Starting NGG was pyrolysed in a single step with the DTG peak centered at 304°C. In the instance of the IBU/NGG blank sample, there were three major mass loss steps (with DTG maxima at 242°C, 270°C and 587°C), apart from the water loss at around 50°C. The absence of a major feature around 450°C, typical for IBU, suggests that the drug may be pyrolysed together with NGG (around 250°C) thus lowering the biopolymer decomposition temperature. Similarly, in the DTG trace of IBU/CGG, the DTG peak that is typical for CGG pyrolysis (centered at 286°C) was shifted to lower temperature (centered at 269°C) and no significant peak typical for IBU pyrolysis was observed. An additional broad peak appeared at around 630°C. These high-temperature DTG features may correspond to thermal events arising from reactions between lower-temperature decomposition byproducts (Leszczyńska et al., 2007). Altered thermal stability of various polymers upon interaction with IBU was reported before and depended on the drug's content and changes in its physical state (Dubernet et al., 1991; Grochowicz and Kierys, 2015). IBU may form different crystal polymorphs upon interaction with polymers and porous solids, and can be present in an amorphous form or as a molecular dispersion within a polymeric matrix (Dubernet et al., 1990; Saravanan et al., 2003; Azais et al., 2006).

3.2.3. IBU/SWy-NGG and SWy-NGG nanocomposites

Upon interaction with NGG, the d-value of Na^+-SWy was enhanced from the initial 12.5 Å to 30 Å and 24 Å for the unwashed and washed SWy-NGG blank samples, respectively (Figs. 3c, 7). Such an increase clearly indicates that NGG is present in the clay mineral's interlayer and that CPN with intercalated structures were obtained. The (001) reflection for the unwashed SWy-NGG-U blank nanocomposite is broad and diffuse, suggesting a partial exfoliation of the clay mineral (Theng, 2012; Bergaya and Lagaly, 2013). The XRD of the washed blank SWy-NGG nanocomposite indicates interlayer spacing of 24 Å. This suggests that upon centrifugation and the simultaneous reduction of the polymer content, clay layers tend to reassemble (Greenland, 1963; Lagaly, 1986). Due to strong interactions between polymer chains and the clay mineral, the latter may partially realign and thus produce intercalated, rather than exfoliated structures. These interactions may involve hydrogen bonding (between –OH groups in the NGG structure and siloxane surface) and ion-dipole interactions (between hydrophilic NGG and the remaining interlayer cations through a water bridge) (Theng, 2012).

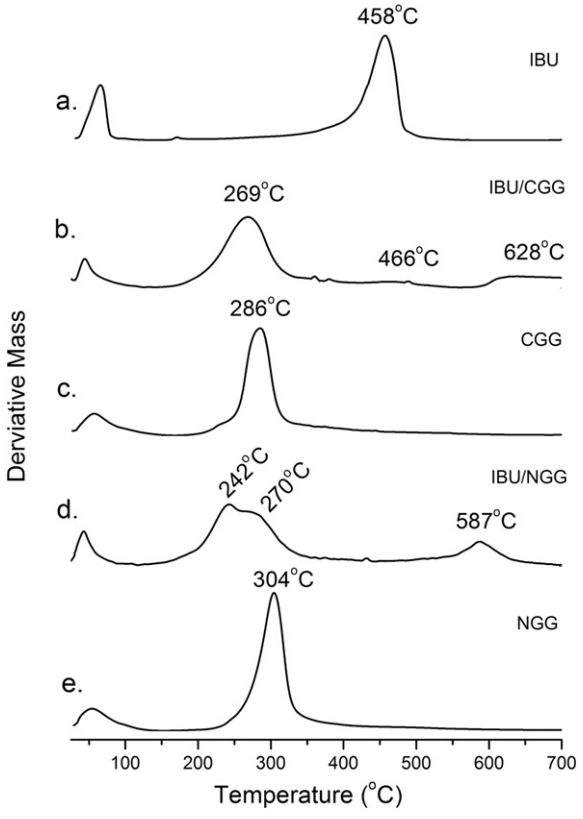

Fig. 5. Differential thermal gravimetric (DTG) traces of (a) IBU; (b) IBU/CGG; (c) CGG; (d) IBU/NGG; (e) NGG.

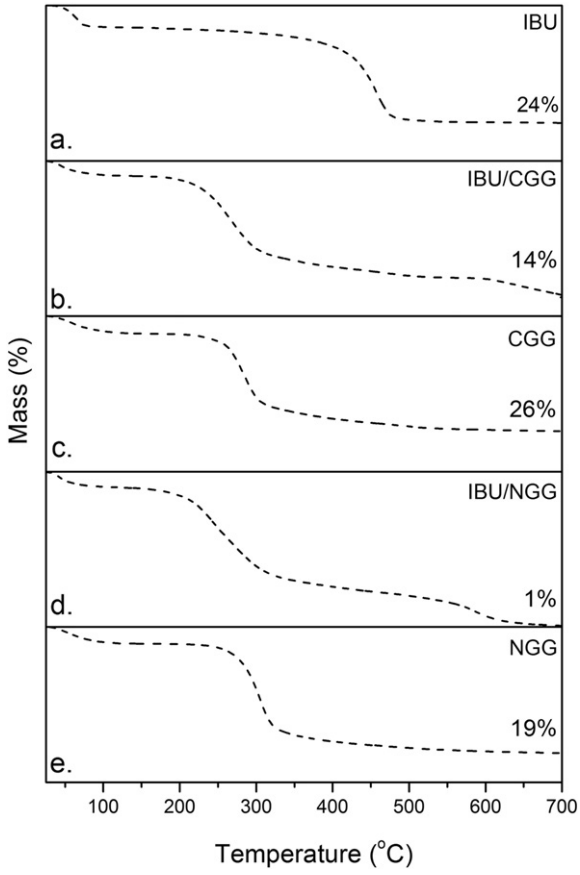

Fig. 6. Thermal gravimetric (TG) traces of (a) IBU; (b) IBU/CGG; (c) CGG; (d) IBU/NGG; (e) NGG. The percentage indicates the remaining sample mass (wt.%) at 700°C.

The XRD pattern of IBU/SWy-NGG-U revealed reflections corresponding to IBU (the most intense at 24 Å) and a lack of a distinct montmorillonite's (001) plane reflection and presence of a broad reflection instead, below the IBU peak at 24 Å (Fig. 7b). The presence of the clay mineral was evidenced by the reflection typical of phyllosilicates at 4.49 Å, which was more pronounced in the XRD pattern of IBU/SWy-NGG. The increasing background, starting from ~13° 2θ is due to an amorphous NGG component. The interlayer space of the centrifuged IBU/SWy-NGG sample is not well defined: the (001) plane reflection is very broad and present at low 2θ angle values. The estimated d_{001} value of 34 Å indicates that NGG was introduced into the interlayer space of Na^+-SWy and that a CPN with the mixed intercalated-exfoliated structure was obtained (Theng, 2012). Additionally, this high interlayer space may suggest that some part of IBU was intercalated together with NGG. The lack of reflections typical for crystalline IBU indicates that the excess of this salt was removed upon centrifugation and the drug molecules were homogenously dispersed within the polymer matrix (Dubernet et al., 1990, 1991). Interestingly, IBU content was reduced only by 7% when compared to IBU/SWy-NGG-U, and this sample exhibits the highest DLE of 70% (Table 2).

DTG and TG traces of the washed IBU/SWy-NGG and unwashed IBU/SWy-NGG-U samples are shown in Figs. 8 and 9, respectively. In case of the latter, apart from the DTG peak with a maximum at 290°C, there is a shoulder centered at 322°C and a series of three minor peaks with

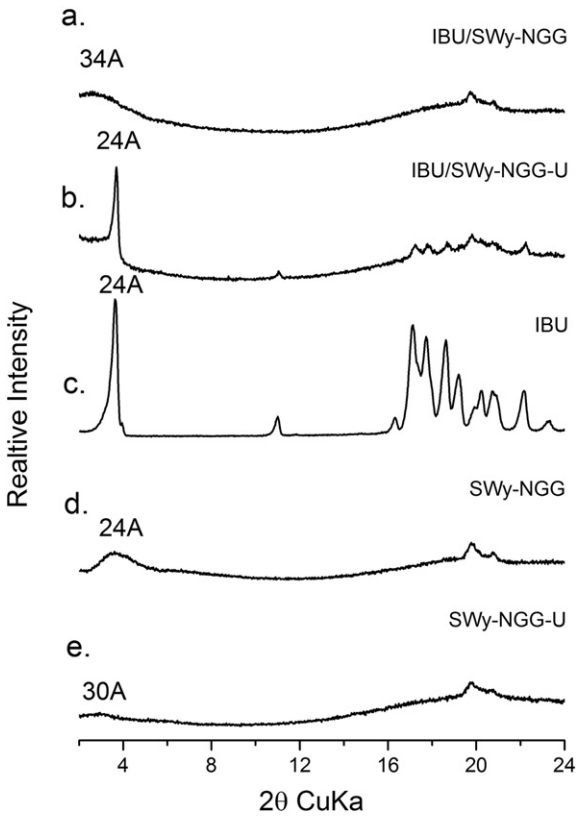

Fig. 7. X-ray diffraction (XRD) patterns (powder mounts) of (a) IBU/SWy-NGG; (b) IBU/SWy-NGG-U; (c) IBU; (d) SWy-NGG; (e) SWy-NGG-U. Intensity scale is unchanged in a, b, d and e subplots.

maxima at 464°C, 543°C and 640°C. Whereas the peak at 464°C corresponds to crystallized IBU, the other features suggest that the drug was dispersed within the polymer matrix, where it interacts with NGG and Mt in varied environments, which affects thermal stabilities of organic nanocomposite constituents (Dubernet et al., 1990; Saravanan et al., 2003). The lack of peaks at 543°C and 640°C for the washed IBU/SWy-NGG suggests that they were due to thermal events related to excess IBU and NGG, which were then removed upon centrifugation. This is in accordance with the DTG trace of IBU/NGG, showing a peak centered at 587°C (Fig. 5d).

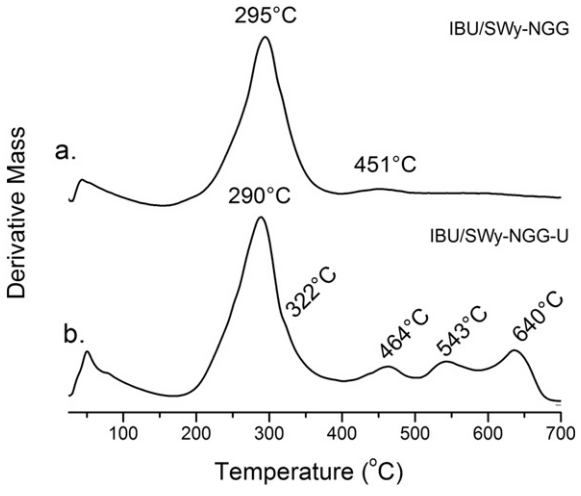

Fig. 8. Differential thermal gravimetric (DTG) traces of (a) IBU/SWy-NGG; (b) IBU/SWy-NGG-U.

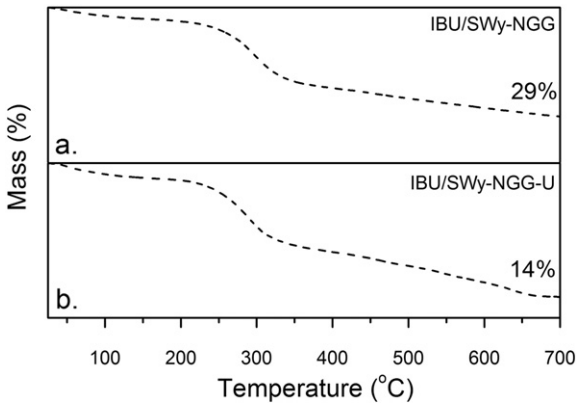

Fig. 9. Thermal gravimetric (TG) traces of (a) IBU/SWy-NGG; (b) IBU/SWy-NGG-U. The percentage indicates the remaining sample mass (wt.%) at 700°C.

3.2.4. SWy-CGG and BV3-CGG Ibuprofen-loaded Nanocomposites

Another set of IBU-loaded materials was prepared with CGG and Na^+-SWy or Na^+-BV3 Mt samples. The choice of CGG was motivated by the fact that its possible interaction with IBU will be enhanced compared to that of NGG: The anionic form of IBU can interact electrostatically with CGG.

XRD patterns (Fig. 10b,e) indicated enhancements of d-values of both IBU/SWy-CGG-U (from 12.5 Å to 14.3 Å) and IBU/BV3-CGG-U (from 12.2 Å to 14.3 Å), comparing to the starting Na^+-SWy and Na^+-BV3, respectively (Fig. 2a,b). This increase indicates that CPN with intercalated structures were obtained. In spite of IBU presence, IBU/SWy-CGG-U exhibited a very similar d-value to blank SWy-CGG (14.5 Å and

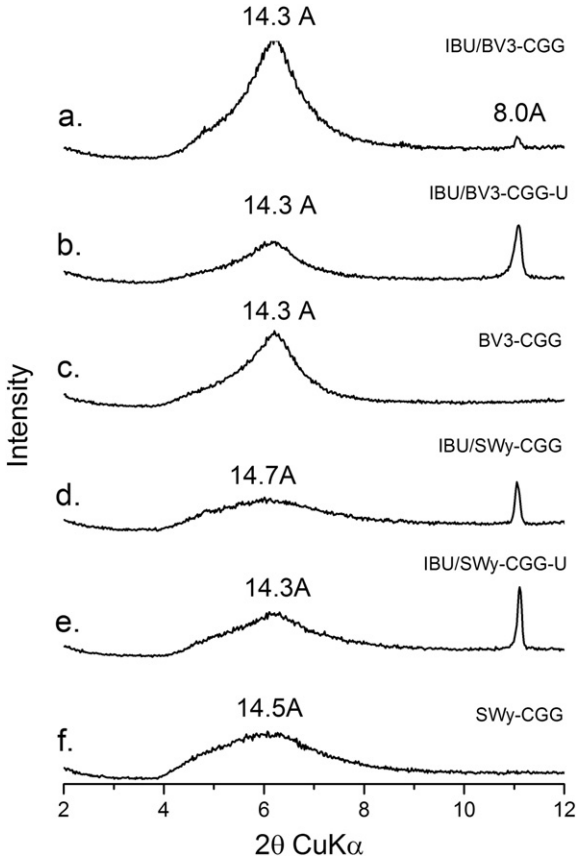

Fig. 10. X-ray diffraction (XRD) patterns (oriented mounts) of (a) IBU/BV3-CGG; (b) IBU/BV3-CGG-U; (c) BV3-CGG; (d) IBU/SWy-CGG; (e) IBU/SWy-CGG-U; (f) SWy-CGG.

14.3 Å, respectively), suggesting that only CGG underwent intercalation between the Mt layers. After washing treatment, the IBU/SWy-CGG sample retained an interlayer space value of 14.7 Å, showing that the CGG in not easily removed by washing with distilled water. The reflections at 8.0 Å, present for both IBU-loaded samples, correspond to crystalline IBU. However, the powder XRD of IBU/SWy-CGG (not shown) revealed that the amount of crystalline IBU has been significantly reduced in comparison with the unwashed IBU/SWy-CGG-U. A similar enhancement of BV3 interlayer space value was revealed for the unwashed IBU/BV3-CGG-U, the washed IBU/BV3-CGG and the blank BV3-CGG (14.3 Å). That indicates stability of the CPN prepared with the Portuguese clay upon washing with water and centrifuging. The minor presence of crystalline IBU is revealed by the reflections at 8.0 Å. Repeatability of the obtained d-value for both Mt samples in the CGG-nanocomposites results from a strong electrostatic interaction between the cationic biopolymer and the negatively charged clay surface, which may affect the ordering of clay layers in the polymeric matrix (Mansa and Detellier, 2013). As such, IBU was most likely dispersed in a polymeric matrix, interacting with both clay mineral layers and polymeric chains.

DTG and TG traces showed a major decomposition feature centered at approximately 280°C for all the samples (Figs. 11, 12). According to the SWy-CGG trace, this peak corresponds to the decomposition of CGG. However, as discussed earlier (IBU/CGG), a certain part of IBU may be also pyrolysed in this temperature range. In the case of IBU/SWy-CGG-U, the relatively small DTG peak with a maximum at 458°C may be attributed to the decomposition of crystalline IBU. The DTG trace of IBU/BV3-CGG-U resembles the trace of the CPN prepared with the reference clay Na^+-SWy. The feature centered at 462°C can be associated with pyrolysis of crystalline IBU, in accordance with the pure IBU DTG trace. The presence of a broad peak with maximum at 597°C (IBU/BV3-CGG-U) again suggests a complex interaction of IBU and CGG on heating.

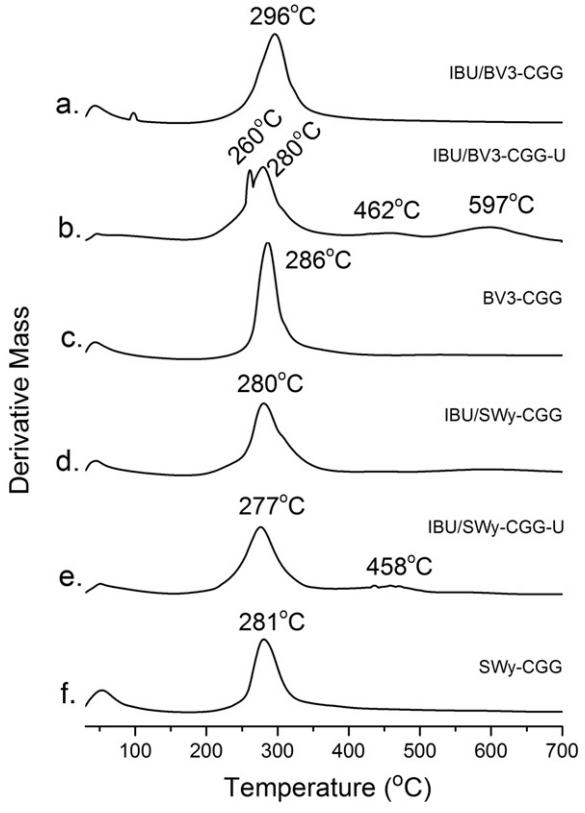

Fig. 11. Differential thermal gravimetric (DTG) traces of (a) IBU/BV3-CGG; (b) IBU/BV3-CGG-U; (c) BV3-CGG; (d) IBU/SWy-CGG; (e) IBU/SWy-CGG-U; (f) SWy-CGG.

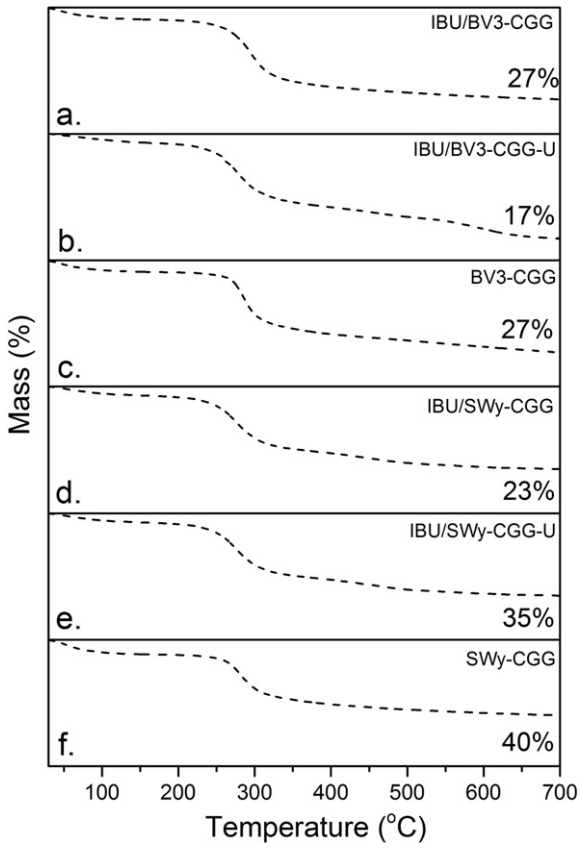

Fig. 12. Thermal gravimetric (TG) traces of (a) IBU/BV3-CGG; (b) IBU/BV3-CGG-U; (c) BV3-CGG; (d) IBU/SWy-CGG; (e) IBU/SWy-CGG-U; (f) SWy-CGG. The percentage indicates the remaining sample mass (wt.%) at 700°C.

3.3. Ibuprofen Release Experiments

3.3.1. Ibuprofen Blank Release Profiles

Initially, behavior of pure IBU blank during release was examined in a pH 7.4 phosphate buffer (Fig. 13a). IBU has a pKa value of 4.91 and low solubility in an acidic medium. On the other hand, the drug is released rapidly at higher pH, reaching 80% cumulative release in the pH 7.4 phosphate buffer within the first 2h. After this time, the concentration of the drug, within the dialysis bag and outside it, became equilibrated.

Release of IBU from the blank Mt samples (IBU/SWy-U and centrifuged IBU/SWy) was studied in a phosphate buffer solution at pH 7.4. The unwashed IBU/SWy-U sample exhibited a very similar drug release pattern as the blank IBU. Despite the fact that some part of IBU was intercalated within the montmorillonite layers, the high drug loading of this sample (68%) hinders any potential effect on sustained release of the drug that could result from its interaction with the clay mineral. In the instance of the centrifuged sample (IBU/SWy), there was a strong decrease in the drug's release rate. Approximately 20% of IBU was released within the first hour, followed by a very slow desorption of the drug from the sample. This indicates that Na^+-SWy can strongly interact with IBU, and this effect is enhanced when a drug loading is low (11%). Since IBU exists prevalently in anionic form at pH 7.4, one possible mechanism of this interaction may be hydrogen bonding between COO^- groups of IBU and –OH groups on montmorillonite's surface (Xu et al., 2006; Zheng et al., 2007). A decreased release rate of the drug from similar complexes have been reported before, where depending on a drug's loading, approximately 40% of IBU was released over 10 hours (Zheng et al., 2007). However, a crucial disadvantage of such systems may be that there is too strong of an interaction between drug and clay mineral, which can prevent the therapeutic levels of drug in the plasma from being reached (Carretero et al., 2006). In case of IBU/NGG

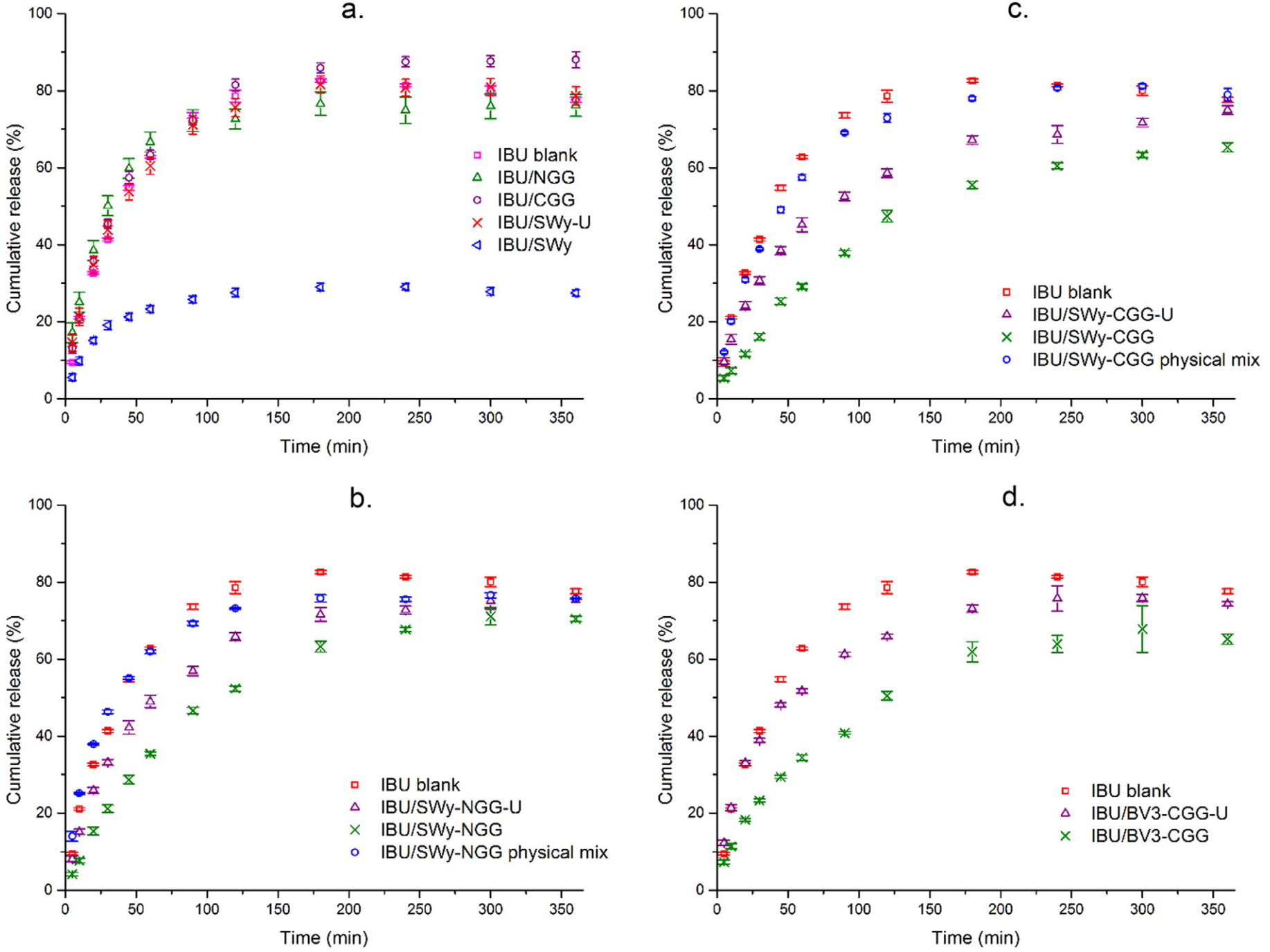

Fig. 13. Cumulative release profiles of IBU-loaded samples in a pH 7.4 phosphate buffer.

and IBU/CGG blanks there was no improvement on IBU release kinetics, despite possible interaction with the drug (Depan et al., 2009). IBU was released quickly within the first 2h. The very rapid swelling of samples in a powdered form was not controlled in any way. As such, the drug can quickly diffuse through the swollen polymer matrix into the release media (Prasad et al., 1998; Das et al., 2006).

3.3.2. IBU/SWy-NGG Release Profiles

The release patterns of the unwashed IBU/SWy-NGG-U and the centrifuged IBU/SWy-NGG samples with DL of 24% and 17%, respectively, (Fig. 13b) showed the improved *in vitro* release properties. The release profiles were additionally compared to a physical mixture of NGG, IBU, and Na^+-SWy, prepared in the same ratio as the IBU/SWy-NGG-U sample (6 : 2 : 1). The plots indicate that there was a slight sustained release-effect observed even for the untreated sample in comparison with the behavior of the physical mixture. The effect was further enhanced in IBU/SWy-NGG sample. This indicates that the sustained release effect was nanocomposite-induced. Most probably, the improved release characteristics of these systems are due to a homogenous dispersion of IBU in the nanocomposite matrix and its increased interaction with NGG and delaminated montmorillonite. IBU can interact with NGG via hydrogen bonding between oxygen atoms in IBU carbonyl groups and plenty of –OH in the biopolymer structure. Additionally, because of the interaction with clay layers and the presence of NGG in the interlayer space of the clay mineral, the extent of biopolymer's swelling may be reduced, and this can also control IBU release (Saravanan et al., 2003; Viseras et al., 2008). Clay-mediated reduced swelling has been proposed as the dominant mechanism that sustains drug release in several systems (Liu et al., 2008; Depan et al., 2009; Wang et al., 2009). These interactions possibly prevent IBU from fast diffusion, which was observed in the case of IBU/NGG blank. The removal of excess crystalline IBU in the case of the centrifuged CPN, and the possible presence of IBU in an amorphous form, as suggested by XRD and TGA, may further contribute to the reduction of IBU release rate. Additionally, this sample exhibits the highest drug loading efficiency (70%).

3.3.3. IBU/SWy-CGG and IBU/BV3-CGG Release Profiles

On the basis of a possible electrostatic interaction of ionized IBU and a positively charged biopolymer, a set of IBU-loaded nanocomposites prepared with CGG and two Mt samples were examined. The IBU release profiles of the unwashed IBU/SWy-CGG-U washed IBU/SWy-CGG samples (Fig. 13c, d) are shown in comparison with a physical mixture of CGG, IBU and Na^+-SWy (4 : 2 : 1 ratio, respectively). A reduced release rate of IBU was observed even for the unwashed sample, as compared to the release pattern of the physical mixture. Again, upon removal of major amount of crystalline IBU, the release was more sustained for IBU/SWy-CGG, with a significantly reduced initial burst release effect. After 90 minutes, 36% less IBU was released from this sample in comparison to the IBU blank. Such a steady release of IBU is desirable in modified drug delivery systems (Viseras et al., 2008). In a first place, homogenous dispersion of IBU in the material and reduced swelling of CGG due to a better defined intercalated structure of the nanocomposite (than for IBU/SWy-NGG) may contribute to further improvements of release parameters. Intercalated structure, with CGG monolayer in the interlayer space, is likely to undergo less swelling in aqueous media than partially exfoliated structure as in case of IBU/SWy-NGG. Such structure, additionally with relatively higher content of smectite than IBU/SWy-NGG, may also contribute to longer diffusion path length of the drug towards the dissolution medium, as well as diffusion of the medium inside the CPN itself, providing a specific tortuous path. This can reduce initial burst release effect of the drug. Depan et al. (2009) attributed initial reduced ibuprofen release rate directly to incorporation of clay mineral and resulting intercalated structure in chitosan-g-lactic/montmorillonite films. Moreover, the electrostatic interaction between COO^- groups of IBU and positively charged aminopropyl functional groups of CGG may play an additional role in a further reduction of the drug release rate, which wasn't observed in case of the IBU/CGG blank due to its rapid swelling and dissolution. Reduced swelling of polymeric matrix, achieved by various strategies, yielded several improved ibuprofen delivery systems (Saravanan et al., 2003; Das et al., 2006; Seeli et al., 2016; Seeli and Prabaharan, 2016).

Table 3
Kinetic release parameters fit using the simplified Higuchi model.

Sample	Model		
	Higuchi Release		
	Equation $Qt = K_H t^{-1/2}$	R^2	K_H
IBU/SWy-NGG	$Q_t = 36.71\ t^{-1/2}$ -3.963	0.975	36.71
IBU/SWy-CGG	$Q_t = 30.62\ t^{-1/2}$ -2.654	0.969	30.62
IBU/BV3-CGG	$Q_t = 32.76\ t^{-1/2} + 0.114$	0.980	32.76

Because of the most pronounced sustained release-properties for the CPN prepared with CGG, similar materials were synthesized using the Portuguese Mt, BV3. The release profiles of the unwashed IBU/BV3-CGG-U and washed IBU/BV3-CGG samples are presented in Fig. 13c, d. Release rate of IBU was also noticeably reduced, when CGG-nanocomposites were prepared with the Portuguese Mt. The initial burst effect was also significantly minimized for the washed sample, IBU/BV3-CGG. This further indicates that nanocomposites prepared with CGG and having a well-defined intercalated structure exhibit a better performance.

The additional advantage of the prepared CPN in comparison with other proposed IBU delivery systems is their very facile and environmentally friendly method of preparation by solvent intercalation in distilled water, based on highly abundant, low-cost, non-toxic and biodegradable (guar gum) resources.

3.3.4. Release Kinetics

The drug release data were fitted to three kinetic models: zero-order, first-order and Higuchi release model, to assess the mechanism of drug release from the CPN. The best fit was obtained for the Higuchi release model: the IBU release rate was proportional to the square root of time (Table 3). Generally, the simplified Higuchi model is applicable when a drug is released from semi-solid and solid matrices and the release is diffusion controlled and is given by the following expression: $f_t = K_H\sqrt{t}$, where f_t is the amount of the drug dissolved, K_H is the Higuchi dissolution constant and t is release time (Higuchi, 1963; Costa et al., 2001; Saravanan et al., 2003). In the case of the CPN, this would indicate that IBU release depends on its diffusion through the swollen polymer matrix, and upon progression in diffusion, the release rate decreases. In accordance with the previous observations, the lowest K_H constant was obtained for IBU-CGG-SWy, which corresponded to the lowest release rate of IBU among the prepared CPN. Release kinetics is strongly dependent on the drug carrier form. Mineral-based IBU release systems in a form of pellets (Campbell et al., 2010) or films (Depan et al., 2009) exhibited extended drug release properties over 10 h and more, thus changing a dosage form from ground powder in case of the prepared CPN can potentially effectuate a further improvement of the IBU release parameters.

4. Conclusions

Treatment with ibuprofen may lead to gastric irritation, and the drug itself has a short biological half-life. Consequently, materials which exhibit sustained release of ibuprofen are desired. In this work, the performance of ibuprofen-loaded guar gum-montmorillonite nanocomposites was assessed *in vitro*, using a membrane diffusion method as a dissolution testing strategy. XRD revealed the intercalated structure of the prepared CPN, with delamination and partial exfoliation. Both neutral guar gum and cationic guar gum were present in the clay mineral spacing, giving rise to ordered structures, particularly in the case of the latter.

Ibuprofen may undergo intercalation into the clay mineral's interlayer space. However, it was not directly evidenced in the interlayer of montmorillonite in the nanocomposite samples. TGA and DTG traces of the CPN indicated altered thermal behavior of ibuprofen upon pyrolysis, suggesting its dispersion in the polymeric matrix, changes in crystallinity, and interaction with both polymer and clay minerals. NMR confirmed the presence of the biopolymers and ibuprofen in the prepared CPN with no evidence of loss in their structural integrity. The release experiments performed in pH 7.4 phosphate buffer indicated that both the neutral guar gum-montmorillonite and cationic guar gum-montmorillonite ibuprofen-loaded nanocomposites exhibited an ability to control the release of the drug. The blank release experiments suggested a nanocomposite-mediated action. Improved properties were demonstrated for both SWy-2 montmorillonite from the Source Clay Repository and natural Portuguese montmorillonite from the Benavila bentonite deposit. In particular, the IBU-CGG-SWy and IBU-CGG-BV3 samples showed the reduction of the initial burst release of ibuprofen and a sustained release of up to 6 hours. The best release parameters of these samples are most likely due to reduced swelling, induced by well-ordered, intercalated structure of the CPN. As the materials were tested in a ground powder form, the sustained release action can be further improved by changing the dosage form, e.g. into compressed tablets or cross-linked beads. Future work should involve studying the release as a function of pH and different ratios of clay mineral to the drug and the biopolymers.

Acknowledgements

This work was financially supported by a Discovery Grant of the Natural Sciences and Engineering Research Council of Canada (NSERC) (CD). The Canada Foundation for Innovation and the Ontario Research Fund are gratefully acknowledged for infrastructure grants to the Center for Catalysis Research and Innovation of the University of Ottawa. This research was partially supported by funds from Geobiotec (UID/GEO/04035/2013, FCT – Fundação para a Ciência e Tecnologia, Portugal). JD acknowledges support from the Erasmus Mundus program, International Master in Advanced Clay Science (IMACS).

Appendix A. Supplementary data

Supplementary data to this article can be found online at http://dx.doi.org/10.1016/j.clay.2016.09.003.

References

Abdeen, R., Salahuddin, N., 2013. Modified Chitosan-Clay Nanocomposite as a Drug Delivery System Intercalation and In Vitro Release of Ibuprofen. J. Chem. N.Y.

Alam, N.H., Meier, R., Schneider, H., Sarker, S.A., Bardhan, P.K., Mahalanabis, D., Fuchs, G.J., Gyr, N., 2000. Partially hydrolyzed guar gum-supplemented oral rehydration solution in the treatment of acute diarrhea in children. J. Pediatr. Gastroenterol. Nutr. 31, 503–507.

Altaf, S.A., Yu, K., Parasrampuria, J., Friend, D.R., 1998. Guar gum-based sustained release diltiazem. Pharm. Res. 15, 1196–1201.

Ambrogi, V., Perioli, L., Ricci, M., Pulcini, L., Nocchetti, M., Giovagnoli, S., Rossi, C., 2008. Eudragit® and hydrotalcite-like anionic clay composite system for diclofenac colonic delivery. Microporous Mesoporous Mater. 115, 405–415.

Arida, A.I., Amro, B., Jaghbir, M., ElAlem, M., Sabri, R., AbuZeid, R., 1999. Development of sustained-release ibuprofen microspheres using solvent evaporation technique. Arch. Pharm. 332, 405–407.

Azais, T., Tourne-Peteilh, C., Aussenac, F., Baccile, N., Coelho, C., Devoisselle, J.M., Babonneau, F., 2006. Solid-state NMR study of ibuprofen confined in MCM-41 material. Chem. Mater. 18, 6382–6390.

Belo, G.M., Diniz Ada, S., Pereira, A.P., 2008. Effect of partially hidrolized guar-gum in the treatment of functional constipation among hospitalized patients. Arq. Gastroenterol. 45, 93–95.

Bergaya, F., Lagaly, G., 2013. Handbook of clay science, Fundamentals. Vol5A Developments of Clay Science, 2nd edition Elsevier.

Bergaya, F., Detellier, C., Lambert, J.F., Lagaly, G., 2013. Introduction to clay–polymer nanocomposites (CPN). In: Bergaya, Lagaly (Eds.), Chapter 13 in Handbook of Clay Science Part A: FundamentalsVol 5A Developments of Clay Science. Elsevier, pp. 655–677.

Brindley, G.W., Brown, G., 1980. Crystal structures of clay minerals and their X-ray identification. Mineralogical Society, London.

Butt, M.S., Shahzadi, N., Sharif, M.K., Nasir, M., 2007. Guar gum: a miracle therapy for hypercholesterolemia, hyperglycemia and obesity. Crit. Rev. Food Sci. Nutr. 47, 389–396.

Campbell, K.T., Craig, D.Q.M., McNally, T., 2010. Ibuprofen-loaded poly(epsilon-caprolactone) layered silicate nanocomposites prepared by hot melt extrusion. J. Mater. Sci. Mater. Med. 21, 2307–2316.

Carignani, E., Borsacchi, S., Geppi, M., 2011. Dynamics by solid-state NMR: detailed study of ibuprofen Na salt and comparison with ibuprofen. J. Phys. Chem. A 115, 8783–8790.

Carrado, K., Decarreau, A., Petit, S., Bergaya, F., Lagaly, G., 2006. Synthetic clay minerals and purification of natural clays. Handbook of Clay Science 1, pp. 115–139.

Carretero, M.I., Pozo, M., 2009. Clay and non-clay minerals in the pharmaceutical industry Part I. Excipients and medical applications. Appl. Clay Sci. 46, 73–80.

Carretero, M., Gomes, C., Tateo, F., 2006. Clays and human health. Handbook of clay science 1, pp. 717–741.

Chaurasia, M., Chourasia, M.K., Jain, N.K., Jain, A., Soni, V., Gupta, Y., Jain, S.K., 2006. Cross-linked guar gum microspheres: a viable approach for improved delivery of anticancer drugs for the treatment of colorectal cancer. AAPS PharmSciTech 7, 74.

Chourasia, M.K., Jain, S.K., 2004. Potential of guar gum microspheres for target specific drug release to colon. J. Drug Target. 12, 435–442.

Costa, P., Manuel, J., Lobo, S., 2001. Modeling and comparison of dissolution profiles. Eur. J. Pharm. Sci. 13, 123–133.

Das, A., Wadhwa, S., Srivastava, A.K., 2006. Cross-linked guar gum hydrogel discs for colon-specific delivery of ibuprofen: Formulation and in vitro evaluation. Drug Deliv. 13, 139–142.

Dawson, J.I., Oreffo, R.O.C., 2013. Clay: New Opportunities for Tissue Regeneration and Biomaterial Design. Adv. Mater. 25, 4069–4086.

Depan, D., Kumar, A.P., Singh, R.P., 2009. Cell proliferation and controlled drug release studies of nanohybrids based on chitosan-g-lactic acid and montmorillonite. Acta Biomater. 5, 93–100.

Droy-Lefaix, M., Tateo, F., 2006. 6 Clays and Clay Minerals as Drugs. Dev. Clay Sci. 1, 743–752.

Dubernet, C., Benoit, J.P., Peppas, N.A., Puisieux, F., 1990. Ibuprofen-Loaded Ethylcellulose Microspheres - Release Studies and Analysis of the Matrix Structure through the Higuchi Model. J. Microencapsul. 7, 555–565.

Dubernet, C., Rouland, J., Benoit, J., 1991. Ibuprofen-loaded ethylcellulose microspheres: Analysis of the matrix structure by thermal analysis. J. Pharm. Sci. 80, 1029–1033.

Gamal-Eldeen, A.M., Amer, H., Helmy, W.A., 2006. Cancer chemopreventive and anti-inflammatory activities of chemically modified guar gum. Chem. Biol. Interact. 161, 229–240.

Gomes, C., Carretero, M.I., Pozo, M., Maraver, F., Cantista, P., Armijo, F., Legido, J.L., Teixeira, F., Rautureau, M., Delgado, R., 2013. Peloids and pelotherapy: Historical evolution, classification and glossary. Appl. Clay Sci. 75-76, 28–38.

Greenland, D.J., 1963. Adsorption of Polyvinyl Alcohols by Montmorillonite. J. Colloid Sci. 18, 647.

Grochowicz, M., Kierys, A., 2015. Thermal characterization of polymer-silica composites loaded with ibuprofen sodium salt. J. Anal. Appl. Pyrolysis 114, 91–99.

Henao, L.J., Mazeau, K., 2009. Molecular modelling studies of clay–exopolysaccharide complexes: soil aggregation and water retention phenomena. Mater. Sci. Eng. C 29, 2326–2332.

Higuchi, T., 1963. Mechanism of sustained-action medication. Theoretical analysis of rate of release of solid drugs dispersed in solid matrices. J. Pharm. Sci. 52, 1145–1149.

Horcajada, P., Serre, C., Vallet-Regí, M., Sebban, M., Taulelle, F., Férey, G., 2006. Metal–organic frameworks as efficient materials for drug delivery. Angew. Chem. 118 (36), 6120–6124.

Krishnaiah, Y.S., Karthikeyan, R.S., Gouri Sankar, V., Satyanarayana, V., 2002a. Three-layer guar gum matrix tablet formulations for oral controlled delivery of highly soluble trimetazidine dihydrochloride. J. Control. Release 81, 45–56.

Krishnaiah, Y.S., Satyanarayana, V., Dinesh Kumar, B., Karthikeyan, R.S., 2002b. In vitro drug release studies on guar gum-based colon targeted oral drug delivery systems of 5-fluorouracil. Eur. J. Pharm. Sci. 16, 185–192.

Kuo, D.C., Hsu, S.P., Chien, C.T., 2009. Partially hydrolyzed guar gum supplement reduces high-fat diet increased blood lipids and oxidative stress and ameliorates FeCl3-induced acute arterial injury in hamsters. J. Biomed. Sci. 16, 15.

Lagaly, G., 1986. Interaction of Alkylamines with Different Types of Layered Compounds. Solid State Ionics 22, 43–51.

Lambert, J.-F., Bergaya, F., 2013. Smectites Polymer Nanocomposites. In: Bergaya, Lagaly (Eds.), Chapter 13.1 in Handbook of Clay Science. Part A: FundamentalsVol 5A Developments of Clay Science. Elsevier, pp. 679–697.

Leszczyńska, A., Njuguna, J., Pielichowski, K., Banerjee, J., 2007. Polymer/montmorillonite nanocomposites with improved thermal properties: Part I. Factors influencing thermal stability and mechanisms of thermal stability improvement. Thermochim. Acta 453, 75–96.

Lichtenstein, D.R., Syngal, S., Wolfe, M.M., 1995. Nonsteroidal Antiinflammatory Drugs and the Gastrointestinal-Tract - the Double-Edged-Sword. Arthritis Rheum. 38, 5–18.

Liu, K.H., Liu, T.Y., Chen, S.Y., Liu, D.M., 2008. Drug release behavior of chitosan-montmorillonite nanocomposite hydrogels following electro stimulation. Acta Biomater. 4, 1038–1045.

Mansa, R., Detellier, C., 2013. Preparation and Characterization of Guar-Montmorillonite Nanocomposites. Materials 6, 5199–5216.

Mansa, R., Huang, C.-T., Quintela, A., Rocha, F., Detellier, C., 2015. Preparation and characterization of novel clay/PLA nanocomposites. Appl. Clay Sci. 115, 87–96.

Marchal-Heussler, L., Maincent, P., Hoffman, M., Spittler, J., Couvreur, P., 1990. Antiglaucomatous activity of betaxolol chlorhydrate sorbed onto different isobutylcyanoacrylate nanoparticle preparations. Int. J. Pharm. 58, 115–122.

Martins, V., Dubert, J., Jouanneau, J.-M., Weber, O., da Silva, E.F., Patinha, C., Dias, J.M.A., Rocha, F., 2007. A multiproxy approach of the Holocene evolution of shelf–slope circulation on the NW Iberian Continental Shelf. Mar. Geol. 239, 1–18.
Mathur, N., 2011. Industrial galactomannan polysaccharides. CRC Press.
Mcginity, J.W., Lach, J.L., 1977. Sustained-Release Applications of Montmorillonite Interaction with Amphetamine Sulfate. J. Pharm. Sci. 66, 63–66.
More, J., Benazet, F., Fioramonti, J., Droylefaix, M.T., 1987. Effects of Treatment with Smectite on Gastric and Intestinal Glycoproteins in the Rat - a Histochemical-Study. Histochem. J. 19, 665–670.
Norrish, K., Quirk, J.P., 1954. Crystalline Swelling of Montmorillonite - Use of Electrolytes to Control Swelling. Nature 173, 255–256.
Oze, C., Bird, D.K., Fendorf, S., 2007. Genesis of hexavalent chromium from natural sources in soil and groundwater. Proc. Natl. Acad. Sci. U. S. A. 104, 6544–6549.
Pang, J.M., Luan, Y.X., Li, F.F., Cai, X.Q., Du, J.M., Li, Z.H., 2011. Ibuprofen-loaded poly(lactic-co-glycolic acid) films for controlled drug release. Int. J. Nanomedicine 6, 659–665.
Park, S.-J., Seo, D.-I., Lee, J.-R., 2002. Surface modification of montmorillonite on surface acid–base characteristics of clay and thermal stability of epoxy/clay nanocomposites. J. Colloid Interface Sci. 251, 160–165.
Porubcan, L.S., Serna, C.J., White, J.L., Hem, S.L., 1978. Mechanism of Adsorption of Clindamycin and Tetracycline by Montmorillonite. J. Pharm. Sci. 67, 1081–1087.
Prabaharan, M., 2011. Prospective of guar gum and its derivatives as controlled drug delivery systems. Int. J. Biol. Macromol. 49, 117–124.
Prasad, Y.V., Krishnaiah, Y.S., Satyanarayana, S., 1998. In vitro evaluation of guar gum as a carrier for colon-specific drug delivery. J. Control. Release 51, 281–287.
Rebelo, M., Rocha, F., da Silva, E.F., 2010. Mineralogical and physicochemical characterization of selected Portuguese Mesozoic-Cenozoic muddy/clayey raw materials to be potentially used as healing clays. Clay Miner. 45, 229–240.
Ribeiro, L.N., Alcântara, A.C., Darder, M., Aranda, P., Araújo-Moreira, F.M., Ruiz-Hitzky, E., 2014. Pectin-coated chitosan–LDH bionanocomposite beads as potential systems for colon-targeted drug delivery. Int. J. Pharm. 463, 1–9.
Rojas, R., Palena, M.C., Jimenez-Kairuz, A.F., Manzo, R.H., Giacomelli, C.E., 2012. Modeling drug release from a layered double hydroxide-ibuprofen complex. Appl. Clay Sci. 62-63, 15–20.
Roussel, H., Waterlot, C., Pelfrene, A., Pruvot, C., Mazzuca, M., Douay, F., 2010. Cd, Pb and Zn Oral Bioaccessibility of Urban Soils Contaminated in the Past by Atmospheric Emissions from Two Lead and Zinc Smelters. Arch. Environ. Contam. Toxicol. 58, 945–954.
Ruiz-Hitzky, E., Aranda, P., Darder, M., Fernandes, F.M., 2013. Fibrous clay mineral–polymer nanocomposites. In: Bergaya, Lagaly (Eds.), Chapter 13.3.4. in Handbook of Clay Science. Part A: FundamentalsVol 5A Developments of Clay Science. Elsevier, pp. 731–735.
Saravanan, M., Bhaskar, K., Rao, G.S., Dhanaraju, M.D., 2003. Ibuprofen-loaded ethylcellulose/polystyrene microspheres: an approach to get prolonged drug release with reduced burst effect and low ethylcellulose content. J. Microencapsul. 20, 289–302.
Schoen, R.T., Vender, R.J., 1989. Mechanisms of Nonsteroidal Anti-Inflammatory Drug-Induced Gastric Damage. Am. J. Med. 86, 449–458.
Seeli, D.S., Prabaharan, M., 2016. Guar gum succinate as a carrier for colon-specific drug delivery. Int. J. Biol. Macromol. 84, 10–15.
Seeli, D.S., Dhivya, S., Selvamurugan, N., Prabaharan, M., 2016. Guar gum succinate-sodium alginate beads as a pH-sensitive carrier for colon-specific drug delivery. Int. J. Biol. Macromol. 91, 45–50.
Sen, G., Mishra, S., Jha, U., Pal, S., 2010. Microwave initiated synthesis of polyacrylamide grafted guar gum (GG-g-PAM)-Characterizations and application as matrix for controlled release of 5-amino salicylic acid. Int. J. Biol. Macromol. 47, 164–170.
Shen, J., Burgess, D.J., 2013. In vitro dissolution testing strategies for nanoparticulate drug delivery systems: recent developments and challenges. Drug Deliv. Transl. Res. 3, 409–415.
Singh, R., Maity, S., Sa, B., 2014. Effect of ionic crosslink on the release of metronidazole from partially carboxymethylated guar gum tablet. Carbohydr. Polym. 106, 414–421.
Soppimath, K.S., Kulkarni, A.R., Aminabhavi, T.M., 2001. Chemically modified polyacrylamide-g-guar gum-based crosslinked anionic microgels as pH-sensitive drug delivery systems: preparation and characterization. J. Control. Release 75, 331–345.
Stewart, M., Jardine, P.M., Barnett, M., Mehlhorn, T., Hyder, L., McKay, L., 2003. Influence of soil geochemical and physical properties on the sorption and bioaccessibility of chromium (III). J. Environ. Qual. 32, 129–137.
Takahashi, T., Yokawa, T., Ishihara, N., Okubo, T., Chu, D.C., Nishigaki, E., Kawada, Y., Kato, M., Raj Juneja, L., 2009. Hydrolyzed guar gum decreases postprandial blood glucose and glucose absorption in the rat small intestine. Nutr. Res. 29, 419–425.
Tan, D., Yuan, P., Annabi-Bergaya, F., Yu, H., Liu, D., Liu, H., He, H., 2013. Natural halloysite nanotubes as mesoporous carriers for the loading of ibuprofen. Microporous Mesoporous Mater. 179, 89–98.
Tan, D., Yuan, P., Annabi-Bergaya, F., Liu, D., Wang, L., Liu, H., He, H., 2014. Loading and in vitro release of ibuprofen in tubular halloysite. Appl. Clay Sci. 96, 50–55.
Theng, B.K.G., 2012. Formation and properties of clay-polymer complexes. Elsevier.
Tiwari, A., Prabaharan, M., 2010. An amphiphilic nanocarrier based on guar gum-graft-poly(epsilon-caprolactone) for potential drug-delivery applications. J. Biomater. Sci. Polym. Ed. 21, 937–949.
Toti, U.S., Aminabhavi, T.M., 2004. Modified guar gum matrix tablet for controlled release of diltiazem hydrochloride. J. Control. Release 95, 567–577.
Tripathy, S., Das, M., Sing, C., 2013. Guar gum: present status and applications. J. Pharm. Sci. Innov. 2, 24–28.
United States Pharmacopeia-National Formulary, 2012. USP 35-NF 30. Second Supplement to USP 35–NF 30. Chemical Tests / ⟨232⟩ Elemental Impurities—Limits 5633–5634.
Van de Wiele, T.R., Oomen, A.G., Wragg, J., Cave, M., Minekus, M., Hack, A., Cornelis, C., Rompelberg, C.J.M., De Zwart, L.L., Klinck, B., Van Wijnen, J., Verstraete, W., Sips, A.J.A.M., 2007. Comparison of five in vitro digestion models to in vivo experimental results: Lead bioaccessibility in the human gastrointestinal tract. J. Environ. Sci. Health A 42, 1203–1211.
Velde, B., Meunier, A., 2008. Plants and Soil Clay Minerals. The Origin of Clay Minerals in Soils and Weathered Rocks. Springer, pp. 241–281.
Viseras, C., Aguzzi, C., Cerezo, P., Bedmar, M.C., 2008. Biopolymer-clay nanocomposites for controlled drug delivery. Mater. Sci. Technol. Lond. 24, 1020–1026.
Wang, Q.S., Cui, Y.L., Zhang, Y., Zhang, Y.B., Gao, X.M., 2009. Preparation and evaluation of chitosan-coated alginate/gelatin sustained releasing microspheres containing berberine hydrochloride in vitro. 2009 3rd International Conference on Bioinformatics and Biomedical Engineering vols. 1-11, pp. 1003–1006.
Wilson, C.G., Washington, N., Greaves, J.L., Kamali, F., Rees, J.A., Sempik, A.K., Lampard, J.F., 1989. Bimodal Release of Ibuprofen in a Sustained-Release Formulation - a Scintigraphic and Pharmacokinetic Open Study in Healthy-Volunteers under Different Conditions of Food-Intake. Int. J. Pharm. 50, 155–161.
Wolfe, M.M., Lichtenstein, D.R., Singh, G., 1999. Gastrointestinal toxicity of nonsteroidal antiinflammatory drugs. N. Engl. J. Med. 340, 1888–1899.
Wragg, J., Cave, M., Basta, N., Brandon, E., Casteel, S., Denys, S., Gron, C., Oomen, A., Reimer, K., Tack, K., 2011. An inter-laboratory trial of the unified BARGE bioaccessibility method for arsenic, cadmium and lead in soil. Sci. Total Environ. 409, 4016–4030.
Xu, S.W., Zheng, J.P., Tong, L., Yao, K.D., 2006. Interaction of functional groups of gelatin and montmorillonite in nanocomposite. J. Appl. Polym. Sci. 101, 1556–1561.
Young, S.L., Sherman, P.W., Lucks, J.B., Pelto, G.H., 2011. Why on Earth?: Evaluating Hypotheses About the Physiological Functions of Human Geophagy. Q. Rev. Biol. 86, 97–120.
Yuan, P., Tan, D., Annabi-Bergaya, F., 2015. Properties and applications of halloysite nanotubes: recent research advances and future prospects. Appl. Clay Sci. 112, 75–93.
Zheng, J.P., Luan, L., Wang, H.Y., Xi, L.F., Yao, K.D., 2007. Study on ibuprofen/montmorillonite intercalation composites as drug release system. Appl. Clay Sci. 36, 297–301.